Coexistence of Ballistic Transport, Diffusion, and Localization in Surface Disordered Waveguides

J. A. Sánchez-Gil
Instituto de Estructura de la Materia, Consejo Superior de Investigaciones Científicas, Serrano 121, 28006 Madrid, Spain

V. Freilikher
The Jack and Pearl Resnick Institute of Advanced Technology, Department of Physics, Bar-Ilan University, Ramat-Gan 52900, Israel

I. Yurkevich
School of Physics and Space Research, University of Birmingham, Edgbaston, Birmingham B15 2TT, United Kingdom

A. A. Maradudin
Department of Physics and Astronomy and Institute for Surface and Interface Science, University of California, Irvine, California 92697
(Received 17 July 1997)

A new regime in the transmission of waves through disordered waveguides is predicted, according to which ballistic, diffusive, and localized modes coexist within the same scale length, due to the surface-type disorder. This entangled regime is confirmed by the different behaviors of the transmitted intensities, obtained by means of numerical simulations based on invariant embedding equations for the reflection and transmission amplitudes. Also, an anomalous conductance crossover from quasiballistic transport to localization is encountered. [S0031-9007(97)05185-5]

PACS numbers: 41.20.Jb, 42.25.Bs, 72.10.Fk, 73.23.–b

The statistical properties of the transmission through a disordered waveguide constitutes a long standing problem that has attracted much attention in recent years from both theoretical and experimental standpoints. Its formulation concerns classical (electromagnetic, acoustic, elastic, gravity, etc.) [1,2] and quantum (electrons) waves alike [3,4]. In either case, it has been shown that the interference of multiply scattered waves is crucial to several phenomena such as weak [1,5,6] and strong (Anderson) [1–4,7,8] localization, intensity correlations [9,10], and universal conductance fluctuations [11]. With regard to classical waves, the problem arises naturally in the characterization of transport properties related to, for instance, optical waveguides and fibers, remote sensing, radiowave propagation, sonar, shallow water waves, and geophysical probing (cf. Refs. [1,2] and references therein). On the other hand, it describes as well the electronic transport in mesoscopic systems [4], being especially relevant to conductance in nanowires [12–14].

A serious theoretical breakthrough in the understanding of the problem occurred when the powerful technique of random matrix theory was applied [15,16]. In the course of the mathematical description of an N-mode waveguide, the random matrix appears in a natural manner as an $N \times N$ matrix of transmission amplitudes t_{nm}. Then the following three types of transmittances can be defined [17]:

$$T_{nm} = |t_{nm}|^2, \qquad T_n = \sum_m T_{nm}, \qquad g = \sum_n T_n . \quad (1)$$

The first one, T_{nm}, measures the coupling between nth incoming and mth outgoing channels (speckle pattern). T_n is the entire transmitted power for the nth incident mode. The last one, g, averages this power over all N incoming channels and corresponds to the dimensionless conductance for electrons. For a waveguide with bulk disorder these entities behave in a similar way. Because of the strong intermode mixing, the incident waves lose their memory after a few scatterings, which means that for waveguides longer than a few scattering lengths l all information about the n dependence is washed out. Therefore all modes switch at $L \sim l$ from the quasiballistic regime to the diffusive one. This shows up in the existence of one universal length scale for all transmittances. This scale is referred to as the localization length and is believed to be equal to Nl. For waveguide lengths shorter than the localization length ($L \ll Nl$) the transmittances have Rayleigh (T_{nm}) or Gaussian (T_n, g) statistics [17–20]. Upon increasing the length ($L \gg Nl$) we observe a crossover to the log-normal distribution which is characteristic for the localized regime. This allows us to state that all channels are equal and undergo the same changes with the increase of the system size.

The goal of the present Letter is to study the differences which occur as far as surface scattering is concerned. Naive considerations would suggest that if we introduce a localization length (which obviously must be much larger than that for the bulk scattering), we should just rescale the well known results leaving the rest unchanged. However,

 0031-9007/98/80(5)/948(4)$15.00

this is not the case: Interference effects display themselves earlier than complete mixing occurs. Some modes become localized well before the intermode coupling involves the other modes into diffusion. Therefore, a waveguide with a random rough surface gives us an example when the symmetry between channels is broken and we can observe all three regimes coexisting at the same system size.

To analyze the problem we derive the invariant embedding equations for the matrices of the reflection and transmission amplitudes following the method suggested in [8]. For a waveguide with a rough surface of length L along its axis (x axis), we obtain the following first-order nonlinear matrix equations:

$$\frac{dr}{dL} = \frac{i}{2}(e^{-ikL} + re^{ikL})\,v(e^{-ikL} + e^{ikL}r), \quad (2)$$

$$\frac{dt}{dL} = \frac{i}{2}te^{ikL}\,v(e^{-ikL} + e^{ikL}r). \quad (3)$$

Here r and t are $N \times N$ matrices of reflection and transmission amplitudes defined through the asymptotics of the scattered field:

$$\Psi_n(x > L, \mathbf{r}) = \frac{1}{\sqrt{k_n}}\chi_n(\mathbf{r})e^{-ik_n x} + \sum_m \frac{1}{\sqrt{k_m}}\chi_m(\mathbf{r})e^{ik_m x}r_{nm}; \quad (4)$$

$$\Psi_n(x < 0, \mathbf{r}) = \sum_m \frac{1}{\sqrt{k_m}}\chi_m(\mathbf{r})e^{-ik_m x}t_{nm}. \quad (5)$$

The $\chi_n's$ are N transverse $[\mathbf{r} \equiv (y, z)]$ eigenfunctions corresponding to the N longitudinal wave numbers k_n, $k = \mathrm{diag}(k_1, \ldots, k_N)$. Scattering is described by the "impurity matrix" v, constructed as follows:

$$v_{nm} = \oint ds\,\phi_m(s)\xi(L, s)\phi_n(s), \quad (6)$$

where s is the arc length along the perimeter of the waveguide cross section, $\phi_n(s)$ is the normal derivative of $\chi_n(\mathbf{r})$ evaluated at the inner surface S of the waveguide,

$$\phi_n(s) = \frac{1}{\sqrt{k_n}}\left[\frac{\partial\chi_n(\mathbf{r})}{\partial\mathbf{r}}\right]_{\mathbf{r}\subset S}, \quad (7)$$

and $\xi(x, \mathbf{r})$ is the random deviation of the surface profile from the translationally invariant unperturbed one.

For the numerical simulations we choose the simplest geometry: two parallel planes $z = 0$ and $z = d$ with a 1D deviation $\xi = \xi(x)$ at one plane ($z = 0$) only. In this case the transverse eigenfunctions acquire the form

$$\chi_n(z) = \sqrt{\frac{2}{d}}\sin(\kappa_n z), \qquad \kappa_n = \frac{\pi n}{d}, \qquad k_n = \sqrt{\left(\frac{\omega}{c}\right)^2 - \kappa_n^2}, \quad (8)$$

and the impurity matrix becomes

$$v_{nm}(L) = \frac{2}{d}\frac{\kappa_n\kappa_m}{\sqrt{k_n k_m}}\xi(L). \quad (9)$$

Our numerical treatment is based on Monte Carlo simulations combined with the 6th-order Runge-Kutta method for solving the system of differential Eqs. (2)–(3). The matrices of reflection and transmission amplitudes are calculated as functions of the length L for each realization $\xi(x)$ of an ensemble of randomly rough surface profiles. These realizations are numerically generated assuming zero-mean Gaussian statistics (δ being the rms height) and a Gaussian correlation function (a being the correlation length). The mean values and fluctuations of the relevant physical quantities are then obtained by ensemble averaging over N_p surface profiles.

In Fig. 1 the $\langle T_{nn}\rangle$ are shown (in a semilog scale) for $0 \geq L/\lambda \geq 1500$ in the case of a waveguide of thickness $d = 4.25\lambda$ supporting $N = 8$ guided modes. Averaging is carried out over $N_p = 2000$ realizations of the surface deviation with $a = 0.2\lambda$ and $\delta = 0.04\lambda$. This plot clearly reveals the drastic differences in behavior for each incoming mode n. On the one hand, the lowest mode $n = 1$ propagates through the waveguide being hardly scattered into other forward or backward propagating modes, so that 85% of the incoming energy remains in the mode after 1500λ. The transmission of the highest incoming mode $n = 8$, on the other hand, decays very rapidly within the 1500λ length due to scattering, in such a way that only less than 1% of the incoming mode leaves the other end of the guide. For the remaining incoming guided modes, the diagonal transmittances exhibit a variety of behaviors bridging the gap between the extreme $\langle T_{nn}\rangle$ for $n = 1$ and 8. Thus, it should be emphasized that surface disorder, in contrast to volume disorder, produces enormous differences in the waveguide transmission properties of each guided mode.

These differences are displayed not only in the magnitude of the transmittances, but mainly in the physical behavior of the propagation of each mode. In Fig. 2, these transport properties are analyzed. Figure 2(a) exhibits

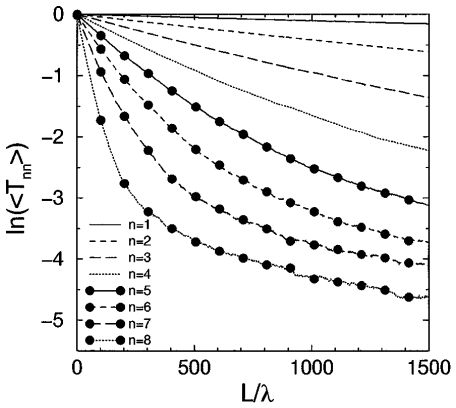

FIG. 1. Logarithm of the averaged diagonal transmission intensities $\langle T_{nn}\rangle$ as a function of the waveguide length L for a width $d/\lambda = 4.25$, supporting 8 modes, with disorder parameters $a/\lambda = 0.2$ and $\delta/\lambda = 0.04$.

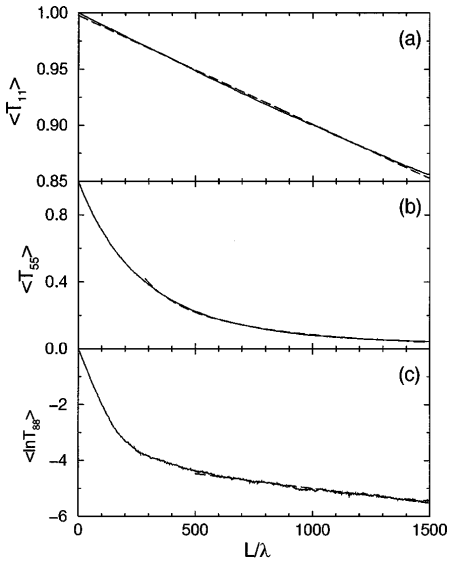

FIG. 2. Averaged diagonal transmission intensities for the same waveguide as in Fig. 1 but only for three modes showing the different transport behaviors: (a) QB for $n = 1$ through a linear fit; (b) D for $n = 5$ through a L^{-1} fit; (c) L for $n = 8$ through a linear fit of $\langle \ln T_{nn} \rangle$.

the *quasiballistic* (QB) transport of the (11)-transmission channel throughout the entire waveguide $L = 1500\lambda$ as revealed by the linear decay $\langle T_{nn} \rangle = 1 - (L/l_{nn}^{\mathrm{QB}})$, with a decay length $l_{11}^{\mathrm{QB}} \approx 10^4\lambda$. The *diffusive* (D) transport of the (55)-transmission channel is shown in Fig. 2(b) through the fit of $\langle T_{55} \rangle$ to the well known hyperbola $\langle T_{nn} \rangle = l_{nn}/L$, from $L \approx 350\lambda$ on, with $l_{55} = 136\lambda$. Finally, the exponential decay $\langle \ln T_{nn} \rangle = -L/l_{nn}^{L}$, associated with *Anderson localization* (L), can be readily recognized in Fig. 2(c) through the L dependence of $\langle \ln T_{88} \rangle$ beyond $L \approx 500\lambda$, yielding a localization length of $l_{88}^{L} = 1007\lambda$. We have also calculated the corresponding relative transmission fluctuations $\delta T_{nn}/\langle T_{nn} \rangle$ [with $\delta T_{nn} = (\langle T_{nn}^2 \rangle - \langle T_{nn} \rangle^2)^{1/2}$] confirming the expected behaviors as shown in Fig. 3: a slow linear increase in the QB regime, $\delta T_{55}/\langle T_{55} \rangle \approx 1$ (speckle pattern) throughout the D region, and growing beyond a variance of unity in the case of the localized mode ($n = 8$). Figures 2 and 3 thus demonstrate the *coexistence of quasiballistic, diffusive, and localized transport* for different incoming channels within the same region of surface disordered waveguide ($500 \leq L/\lambda \leq 1500$). (It should be mentioned that the L regime for the $n = 8$ mode is preceded by a D one, and this in turn by a very short QB one, with the associated QB-D and D-L transitions. The QB-D crossover is also observed for $n = 5$. The D-L crossover in the conductance has been studied with a similar geometry in Ref. [21]; curves similar to those shown in Fig. 1 have been independently reported therein.)

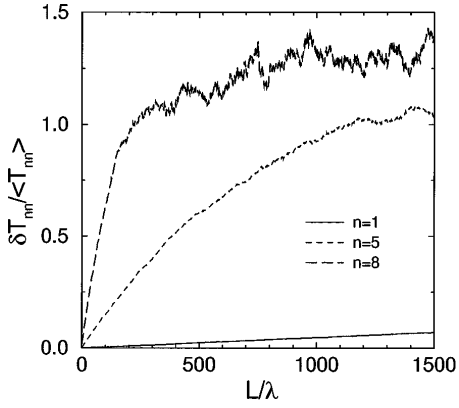

FIG. 3. Normalized fluctuations of the transmission intensities shown in Fig. 2 as functions of the waveguide length L.

This anomalous behavior can be qualitatively interpreted in terms of a rough estimate of the number M_n of scattering events that each mode undergoes along its trajectory within the waveguide. By assuming that the rough boundary rms deviation δ is small compared with the mean waveguide width, the former number is given by

$$M_n = \frac{L\kappa_n}{2dk_n}. \tag{10}$$

In fact, the impurity matrix acting as the scattering potential can be written in terms of these numbers as

$$v_{nm} = \frac{8d^2}{L^2}\frac{\xi(L)}{d}(k_n k_m)^{1/2} M_n M_m. \tag{11}$$

In the case of the above calculations, for instance, it turns out that $M_8 = 23.5M_1$, so that $v_{88}/v_{11} = 188$. This factor explains the large differences between the corresponding (11)- and (88)-transmission coefficients, being in reasonable agreement with our numerical results ($l_{88}^{\mathrm{QB}} \approx 5 \times 10^{-3} l_{11}^{\mathrm{QB}}$). Similar scaling differences apply to the remaining transmitted modes.

The interplay between mode conversion and the above mentioned distinct transmission features produced by surface disorder manifests itself also in the total transmission T_n and the dimensionless conductance g. Since every T_{nm} behaves differently [recall that $v_{nm} = (k_m/k_n)^{1/2} \times (M_m/M_n)v_{nn}$], the sum over the nondiagonal terms ($m \neq n$) yields at certain lengths a total transmission where the three regimes are entangled, thus making it unfeasible to define a transport regime. Only when mode coupling is weak and/or the (nm) scaling lengths swap can one assess that the behavior of the total transmission coincides with that of the diagonal transmission. This has been verified in our numerical simulations: Whereas the QB (L) regimes are easily recognized at sufficiently short (large) length scales, the D regime is either observable only within a narrow waveguide length window, or is absent. The entangling of transport regimes due to surface disorder becomes more evident when dealing with the dimensionless conductance, the relevant quantity in the electronic problem. In Fig. 4, its average and fluctuations are depicted both for the 8-mode waveguide studied thus far and for a narrower waveguide (supporting only $N = 4$ guided modes) with a rougher surface ($\delta = 0.08\lambda$). The initial QB linear decay and the long-length L exponential decay are shown in Fig. 4(a)

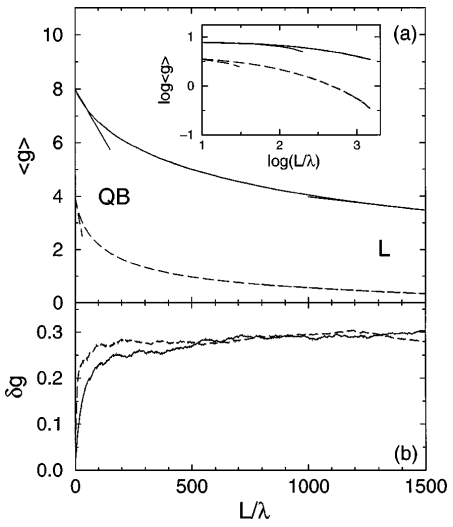

FIG. 4. (a) Averaged conductance through the waveguide used in Fig. 1 (solid curves) and through a narrower waveguide (dashed curves) of width $d/\lambda = 2.25$ (thus supporting only 4 modes) and disorder parameters $a/\lambda = 0.2$ and $\delta/\lambda = 0.08$. The linear (exponential) decays at short (long) lengths define the QB (L) regimes. The inset shows the logarithmic plot. (b) Conductance fluctuations.

through appropriate fits; in between these QB and L regions, $\langle g \rangle$ fails to fit the L^{-1} dependence characteristic of the D regime (this is more clearly observed in the log-plot in the inset). Furthermore, the fluctuations lie below the expected quasi-1D UCF value for such a regime [upper horizontal axis in Fig. 4(b), $\delta g \approx 0.364$, cf. Refs. [11–13]]. Therefore, as far as the conductance is concerned, an anomalously long effective crossover from the QB directly to the L regime can take place, due to the coexistence of QB, D, and L regimes in different transmission channels within the same length scale.

In summary, we have demonstrated the coexistence of QB, D, and L regimes within the same region in the transport of waves through a surface disordered waveguide. This phenomenon manifests itself through both the different behaviors of the T_{nm} (average and fluctuations), and the anomalous QB-L crossover in the conductance that fails to exhibit the D regime in between. Thus the coexistence of regimes can be revealed experimentally by measuring either the transmission intensities of guided microwaves or light (or any other accessible electromagnetic or classical wave), or the anomalous conductance crossover in the electronic problem. In the case of microwaves of $\lambda \sim 1$ cm, waveguides (or tubes [20]) several centimeters wide could be used, consisting of metallic plates one of which, at least, should have irregularities with lateral dimensions of the order of millimeters (for instance, by using aluminum foil). The required waveguide lengths some meters long at which the coexistence is observed can be reduced by making the roughness strength larger than that employed in our calculations. Similar considerations apply to optical waveguides in the micron scale; in fact, the needed surface roughness is present, due to the fabrication process, in typical silica waveguides [22].

J. A. S. G. is grateful to A. García-Martín, J. A. Torres, J. J. Sáenz, and M. Nieto-Vesperinas for valuable discussions. He acknowledges support from the Spanish CSIC, DGES (through Grant No. PB96-0886), and CAM. The work of A. A. M. was supported in part by US-ARO Grant No. DAAH 0-96-1-0187. I. Y. acknowledges support from EPSRC Grant GR/K95505.

[1] *Scattering and Localization of Classical Waves in Random Media*, edited by P. Sheng (World Scientific, Singapore, 1990).
[2] V. Freilikher and S. Gredeskul, Prog. Opt. **30**, 137 (1992).
[3] P. W. Anderson, Phys. Rev. **109**, 1492 (1958).
[4] P. A. Lee and T. V. Ramakrishnam, Rev. Mod. Phys. **57**, 287 (1985); *Mesoscopic Phenomena in Solids*, edited by B. L. Altshuler, P. A. Lee, and R. A. Webb (North-Holland, Amsterdam, 1991).
[5] Y. Kuga and A. Ishimaru, J. Opt. Soc. Am. A **1**, 831 (1984); M. P. van Albada and A. Lagendijk, Phys. Rev. Lett. **55**, 2692 (1985); P. E. Wolf and G. Maret, Phys. Rev. Lett. **55**, 2696 (1985).
[6] K. A. O'Donnell and E. R. Méndez, Opt. Commun. **61**, 91 (1987); M. Nieto-Vesperinas and J. M. Soto-Crespo, Opt. Lett. **12**, 979 (1987).
[7] S. John, Phys. Rev. Lett. **53**, 2169 (1984).
[8] N. Makarov and I. Yurkevich, Sov. Phys. JETP **69**, 628 (1989); V. Freilikher, M. Pustilnik, and I. Yurkevich, Phys. Rev. Lett. **73**, 810 (1994).
[9] B. Shapiro, Phys. Rev. Lett. **57**, 2168 (1986); A. Z. Genack, Phys. Rev. Lett. **58**, 2043 (1987).
[10] T. R. Michel and K. A. O'Donnell, J. Opt. Soc. Am. A **9**, 1374 (1992); M. Nieto-Vesperinas and J. A. Sánchez-Gil, Phys. Rev. B **46**, 3112 (1992); J. Opt. Soc. Am. A **10**, 150 (1993).
[11] R. A. Webb, S. Washburn, C. P. Umbach, and R. B. Laibowitz, Phys. Rev. Lett. **54**, 2696 (1985).
[12] H. Tamura and T. Ando, Phys. Rev. B **44**, 1792 (1991); T. Ando and H. Tamura, Phys. Rev. B **46**, 2332 (1992).
[13] P. García-Mochales, P. A. Serena, N. García, and J. L. Costa-Krämer, Phys. Rev. B **53**, 10 268 (1996).
[14] J. A. Torres and J. J. Sáenz, Phys. Rev. Lett. **77**, 2245 (1996).
[15] K. A. Muttalib, J.-L. Pichard, and A. D. Stone, Phys. Rev. Lett. **59**, 2475 (1987).
[16] C. W. J. Beenakker, Rev. Mod. Phys. **69**, 731 (1997).
[17] S. A. van Langen, P. W. Brouwer, and C. W. J. Beenakker, Phys. Rev. E **53**, 1344 (1996).
[18] I. Edrei, M. Kaveh, and B. Shapiro, Phys. Rev. Lett. **62**, 2120 (1989).
[19] J. F. de Boer, M. C. W. van Rossum, M. P. van Albada, Th. M. Nieuwenhuizen, and A. Lagendijk, Phys. Rev. Lett. **73**, 2567 (1994).
[20] M. Stoytchev and A. Z. Genack, Phys. Rev. Lett. **79**, 309 (1997).
[21] A. García-Martín, J. A. Torres, J. J. Sáenz, and M. Nieto-Vesperinas, Appl. Phys. Lett. **71**, 1912 (1997); Phys. Rev. Lett. (to be published).
[22] F. Ladouceur and L. Poladian, Opt. Lett. **21**, 1833 (1996).